Journal of Applied Polymer Science

Enhanced Microwave Absorbing Properties of Lightweight Films Based on Polyaniline/Aliphatic Polyurethane Composites in X Band

Sofiane Zeghina,[1] Jean-Luc Wojkiewicz,[2,3] Saad Lamouri,[1] Belkacem Belaabed,[1] Nathalie Redon[2,3]

[1]Laboratoire de Chimie Macromoléculaire, Ecole Militaire Polytechnique (EMP), Bordj El Bahri, 16111 Alger Algérie

[2]Université Lille Nord de France, F-59000 Lille, France

[3]Mines Douai, Département Sciences de l'Atmosphère et Génie de l'Environnement (SAGE), 941 rue Charles Bourseul, F-59508 Douai, France

Correspondence to: J.-L. Wojkiewicz (E-mail: jean-luc.wojkiewicz@mines-douai.fr)

ABSTRACT: Polymer blends based on nanostructured polyaniline (PANI) doped with hydrochloric acid (HCl) and para-toluene sulfonic acid (PTSA) introduced into aliphatic polyurethane matrix (PU) are synthesized to produce flexible thin composite films for microwave absorbers. The effects of dopant type, PANI content and film thickness on morphologies, dielectric and microwave absorption properties in the X-band are studied. It reveals that real and imaginary parts of the complex permittivity are proportional to filler concentrations and type of doped PANI. The PANI-PTSA/PU films show higher permittivity and better microwave absorbing properties than PANI-HCl/PU for the same weight fraction of PANI. The minimum reflection loss $RL_{(dB)}$ values for the PANI-PTSA/PU are −37 dB at (20% PANI and 11.6 GHz) and −30 dB at (15% PANI and 11.3 GHz) for thicknesses of 1.2 and 1.6 mm, respectively. These high values of reflection losses make the obtained lightweight and flexible composites promising radar absorbing materials (RAM). © 2014 Wiley Periodicals, Inc. J. Appl. Polym. Sci. **2014**, *131*, 40961.

KEYWORDS: applications; composites; conducting polymers; dielectric properties; polyurethanes

Received 10 January 2014; accepted 4 May 2014

DOI: 10.1002/app.40961

INTRODUCTION

In the last decade, composite blends based on conductive organic/inorganic fillers dispersed in insulating matrix have been widely investigated because of their widespread applications such as electromagnetic shielding (EMI) and electromagnetic static discharge (ESD) with both commercial and defense purpose.[1–3] In the stealth technology of aircraft, advanced composite materials are used as radar absorbing materials (RAM) to attenuate the electromagnetic beam and reduce the radar cross section (RCS).[4] Usually, these materials are obtained by the dispersion of one or more types of absorbing fillers in a matrix. They can be produced in different forms such as paints, sheets, and thin films as single, double or multi-layer.[5] In each application, it is necessary to control precisely the physical properties of the material in terms of permittivity, conductivity and to know their variations with the frequency. This can be achieved by the use of suitable fillers such as conducting, dielectric, or magnetic particles.[6–8] But the mechanical properties of these materials are deteriorated with the rate of loading and the weight of the material becomes incompatible particularly with the aeronautical and aerospace applications.

For these reasons, intrinsically conducting polymers and particularly, polyaniline became a credible alternative. It showed a good thermal and chemical stability and its electronic properties can be tuned easily from insulating to conducting states through chemical process. Many works showed that polyaniline provides materials with high levels of electromagnetic shielding performances at microwave frequencies with a low mass by unit of surface.[9,10] In addition, PANI not only reflects but also absorbs electromagnetic wave, and can reach high levels of shielding performance by the use of different dopant agents such as camphor sulfonic acid, para-toluene sulfonic acid and hydrochloric acid.[11,12] However, the poor mechanical properties and the reduced solubility in common organic solvents of doped PANI could be a barrier to the development of this application. Blending PANI with common polymers surpasses these inconveniences.[13] In this way, the electrical properties of doped PANI can be combined with the mechanical properties of conventional polymers like polyurethane matrix to obtain flexible composites with improved microwave absorption properties.[9] The choice of polyurethane as the elastomeric matrix is due to its favorable properties, which include excellent resistance to aging, water and favorable flame retardant behavior,

allowing its use for aeronautical and naval applications.[14] Several methodologies have been adopted for the preparation of microwave absorbing composites. Usually, it based on the combination of glass fabric composites and polyurethane with conductive fillers to obtain electromagnetic wave absorbing sandwich structures.[15]

The aim of this article is to obtain thin organic lightweight flexible films with better dispersion of PANI nanostructures in the aliphatic PU matrix to improve the electromagnetic properties. The PANI/PU composites were carried during the crosslinking of polyurethane to promote chemical interactions between PANI and PU. First, polyaniline nanostructures were dispersed in hyperbranched hydroxyl-terminated polyester, and then aliphatic isocyanate was added for crosslinking by *in situ* one-shot polymerization process. For comparative study, the PANI/PU composites were synthesized by employing two different types of PANI. The first type was PANI doped hydrochloric acid (PANI-HCl) and second type was PANI-doped para-toluene sulfonic acid (PANI-PTSA). The structure and the morphology of the samples were investigated by FTIR, XRD, SEM, and TEM analysis. The influence of the dopant type, PANI content and film thickness on the electromagnetic properties of composites has been investigated. The results showed that with in situ one-shot polymerization process, the aliphatic polyurethane give higher dielectric and microwave absorption properties with PANI-PTSA than PANI-HCl at film thicknesses below 2 mm, in the X-band (8.2–12.4 GHz), which make them promising materials for microwave absorption.

EXPERIMENTAL

Materials

Hyperbranched hydroxyl-terminated polyester (desmophen 651) and 1,6-hexamethylene aliphatic diisocyanate (desmodur N75) were supplied from Bayer Material Science. Aniline (99% purity) was purchased from Merck. Ammonium peroxydisulfate (99%), ethanol (99%), tetrahydrofuran (99%), and hydrochloric acid (37%) were supplied from Prolabo. PANI-PTSA was purchased from Sigma-Aldrich and PANI-HCl homemade was synthesized according to IUPAC recommendations.[16]

Composite Preparation

To reveal the effect of doping agent on the desired properties, two types of PANI-HCl/PU and PANI-PTSA/PU composites were prepared by dispersing PANI in situ during the progression of the curing of the aliphatic PU. The PANI/PU composites were elaborated with mass content of PANI ranging from 5 to 25 wt % in order to minimize the alteration of the mechanical properties of the PU and to get samples near the percolation threshold value.

First, PANI-HCl and PANI-PTSA were dispersed in THF as solvent separately for 1 h then, the two dispersions were mixed with hyperbranched hydroxyl-terminated polyester resin using ultrasonic bath followed by magnetic stirring in order to improve the dispersion quality for 2 h, then aliphatic diisocyanate 1,6-hexamethylene was added after 30 min while keeping the stirring. The mixtures were deposited in boxes kneaded and dried at 60°C until complete consumption of isocyanate and solvent, the evolution of the polymerization reaction is monitored by FTIR. The obtained flexible films were prepared in a rectangular shape with different thicknesses and appropriate dimensions to be integrated into the wave guide for electromagnetic characterization.

Instrumental Analysis

The chemical structures of PANI-HCl and PANI-PTSA powders were determined by Fourier Transform Infrared (FTIR) spectrometer (Shimadzu 8400S, KBr pellets), the virgin PU and its composite films PANI-HCl/PU and PANI-PTSA/PU were analyzed using attenuated total reflection (ATR-FTIR). The (XRD) analysis of the samples were performed using diffractometer (X'PERT Pro MPD PANalytical), operating at a wavelength of 1.5418 Å, 40 kV, and 40 mA. The morphologies were observed using SEM (Zeiss Supra 40 VP) operating with secondary electrons at 5–20 kV and TEM (Philips EM430) at 300 kV. The (DC) conductivity was measured with a four-probe method using a (Minirosion LTD type BA model). Pellets of compressed PANI-HCl and PANI-PTSA powders were prepared under a pressure of 70 kN with a thickness of 0.7 mm while composites PANI-HCl/PU and PANI-PTSA/PU were measured in the form of thin films.

The reflection coefficient (S_{11}) and the transmission coefficient (S_{21}) were measured by using a Vector Network Analyzer (VNA) type (E8362B Agilent technologies working from 10 MHz to 20 GHz). The rectangular samples ($25 \times 13 \times d$ mm) with different thickness $d = 1.2$, 1.6, and 2 mm of composite were inserted into a standard coaxial sample holder which matches the internal dimensions of X-band (8.2–12.4 GHz) waveguide and they have been placed between the two ports of the network analyzer.[7,17] However, the microwave absorption properties were measured using the same instrument but the rear face of the sample was terminated by a short-circuit that is a perfect conductor in aluminum.

RESULTS AND DICUSSION

Spectroscopy Analysis

Figure 1(a) shows FTIR spectra of HCl and PTSA-doped PANI, which are in agreement with previously reported results.[2,18] Various common absorption bands at 3439, 2924, 1561, 1479, 1298, 1245, 1105, 800, and 501 cm^{-1} are observed in the two cases. The absorption at 3439 cm^{-1} is due to the N–H stretching vibrations. The aromatic C—H is usually observed at 2924 cm^{-1}. The peaks at about 1561 cm^{-1} and 1479 cm^{-1} are related to the quinone structure and benzene ring stretching respectively. The aromatic C—N stretching indicating secondary aromatic amine group is located at 1245−1298 cm^{-1}. The peak at 1105 cm^{-1} is attributed to the deformation of the aromatic C—H of quinoid which is considered as electronic-like bands and is known to be a measurement of the electron delocalization degree in PANI chains.[19] The band at 800 cm^{-1} is attributed to out-of-plane C—H bending. For PANI-doped PTSA, the peak at 1010−1039 cm^{-1} are related to the symmetric stretching of SO_3 group from the dopant molecule.[20] Furthermore, in PANI-doped HCl, the C—Cl stretching peak arises in the region 590−706 cm^{-1}.[21]

On Figure 1(b), the spectra (a–d) represent the temporal evolution of residual isocyanate components upon curing. The

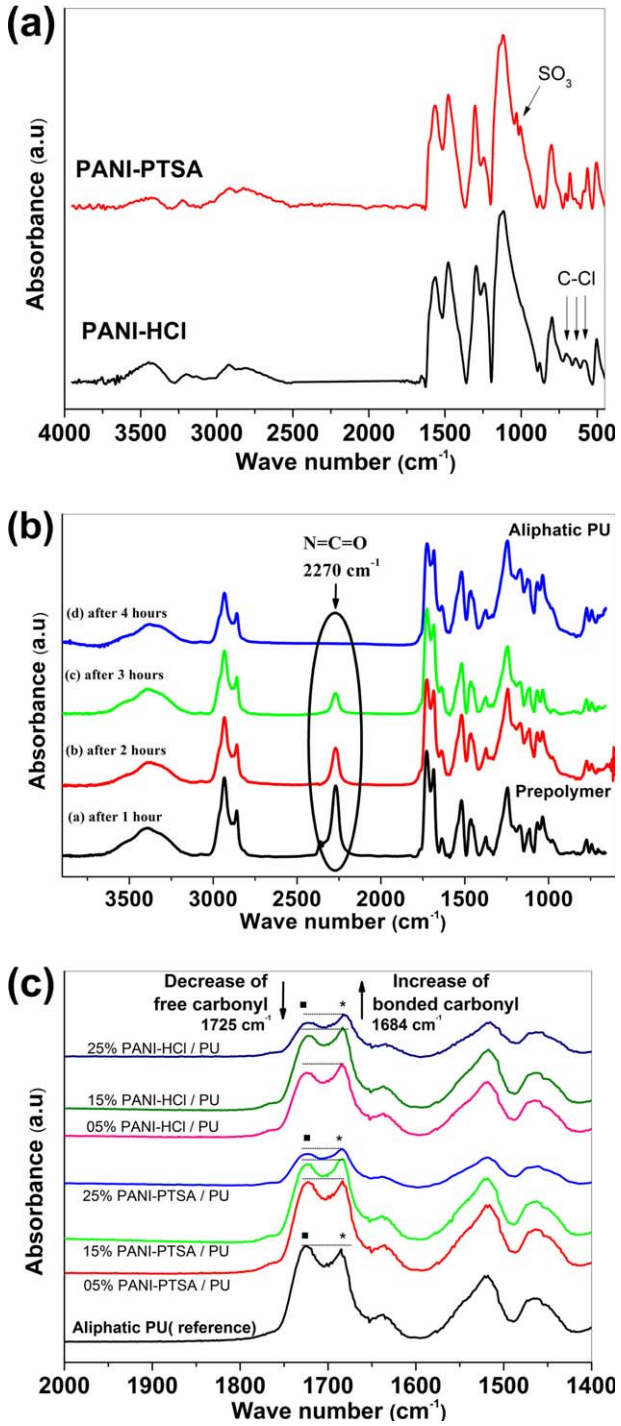

Figure 1. FTIR spectra of: (a) PANI powders, (b) Temporal evolution of isocyanate peak in the condensation reaction of PU and (c) FTIR spectra of virgin PU and PANI/PU composites in the range 1400–2000 cm^{-1}. [Color figure can be viewed in the online issue, which is available at www.interscience.wiley.com.]

aliphatic polyurethane is fully cured after 4 h at 60°C as shown by the strong reduction of the NCO peak at 2270 cm^{-1}. The FTIR spectrum of virgin polyurethane presents bands around 3515 cm^{-1} and 3384 cm^{-1} corresponding to the free and bonded N—H stretching vibrations of urethane, respectively.

Table I. Evolution of Intensity Ratio of (bonded carbonyl/free carbonyl) in PANI/PU Composites Compared with Virgin PU

Composition	PANI rate (%)	Intensity ratio (bonded carbonyl at 1684 cm^{-1}/ free carbonyl at 1725 cm^{-1})
Virgin PU	0	0.9068
PANI-PTSA/PU composites	5	1.0040
	15	1.0478
	25	1.0610
PANI-HCl/PU composites	5	1.0338
	15	1.0437
	25	1.0536

The CH_2 symmetric and anti-symmetric stretching vibrations are located at 2934 cm^{-1} and 2859 cm^{-1}. The intensive peaks at 1725 cm^{-1} and 1684 cm^{-1} are respectively assigned to the free carbonyl (C═O) and bonded carbonyl (C═O) of urethane stretching vibrations. The absorption at 1466 cm^{-1} and 1379 cm^{-1} are attributed to (CH_2). The peak related to the valence vibration ν(C—N) and deformation vibration δ(N—H) appears at 1524 cm^{-1}.[22] The existence of bands for (N—H) and (C═O) of the urethane confirms that the reaction of polymerization had taken place.[23]

Considering the structure and the chemical nature of each component of the composites, specific interactions of the hydrogen bonding type are likely developed between the PANI and PU. In order to check the existence of such interactions in PANI/PU composites, (ATR-FTIR) spectra are inspected in the range between 1400 cm^{-1} and 2000 cm^{-1}, which corresponds to the stretching vibration of the carbonyl groups (C═O). On Figure 1(c), it reveals that by increasing PANI content in both composites PANI-HCl/PU and PANI-PTSA/PU, an increase in absorption band intensity of bonded (C═O) groups at 1684 cm^{-1} accompanied by a decrease in the intensity band of free (C═O) groups at 1725 cm^{-1} are observed, contrary to the virgin polyurethane which has the intensity of free carbonyl superior to those of bonded carbonyl as shown on Table I. These results indicate the existence of specific interactions between the (N—H) groups of PANI and the (C═O) groups of polyurethane, which are mainly attributed to the formation of the hydrogen bonding.[24]

XRD Analysis

The XRD patterns of doped PANI with HCl and PTSA are shown in Figure 2(a). Doped PANI is a heterogeneous system consisting of a moderately crystalline region dispersed in an amorphous phase which may be important for charge localization/interfacial polarization and electromagnetic wave absorbing properties. The HCl-doped PANI presents three main reflections located at $2\theta = 14.6°$, 20.6°, and 25° which correspond to the orthorhombic structure of emeraldine salt. While PTSA-doped

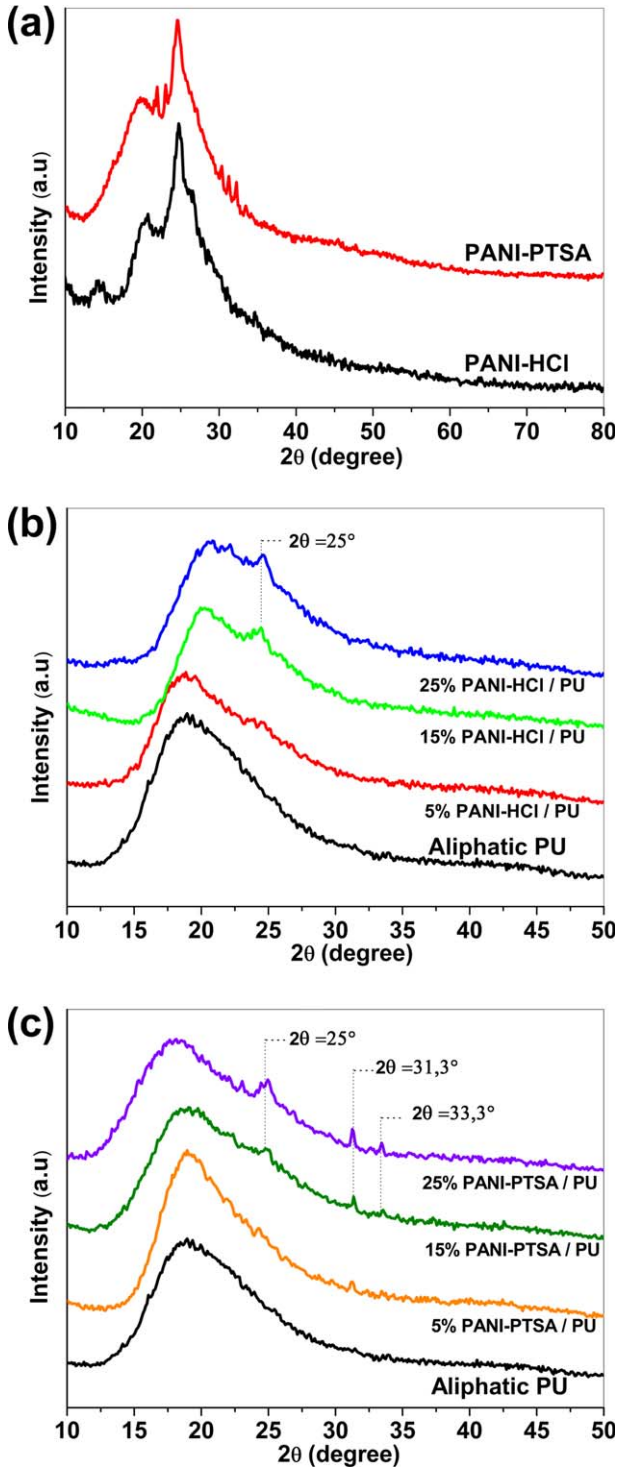

Figure 2. XRD patterns of (a) PANI powders doped HCl and PTSA, and its composites: (b) PANI-HCl/PU and (c) PANI-PTSA/PU at different amount of PANI. [Color figure can be viewed in the online issue, which is available at www.interscience.wiley.com.]

PANI shows more than three main reflection peaks localized at $2\theta = 20.6°$, 21.9°, 23°, 25°, 30.4°, 31.3°, and 33.3°.[25] This result confirms the higher crystallinity degree of PANI-PTSA compared with PANI-HCl. In both cases of doped PANI, the crystalline phase is confirmed by the presence of a strong peak at

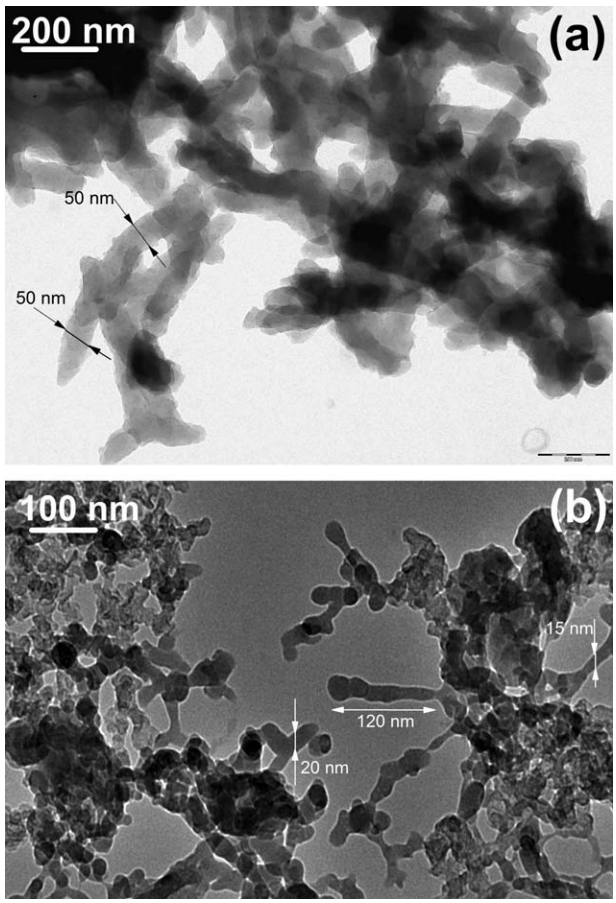

Figure 3. TEM images of nanofibers: (a) PANI-HCl and (b) PANI-PTSA.

$2\theta = 25°$ and the amorphous phase is localized by the small peak observed at $2\theta = 20.6°$.[26]

The aliphatic polyurethane is completely amorphous, as shown by the single broad maximum centered at $2\theta = 19°$. From the X-ray diffraction of PANI/PU composites on Figure 2(b,c), it is found that by increasing PANI-HCl and PANI-PTSA content in composite, the peak at $2\theta = 25°$ appears for composites with a mass fraction of doped PANI above 15%. It indicates an ordering process in the composite chains after this amount of PANI and can be attributed to the percolation phenomena. Other peaks appear at $2\theta = 31.3°$ and $2\theta = 33.3°$ for PANI-PTSA/PU composites indicating better crystallinity for these films.

Morphologies

The morphologies of the doped PANI and their composites were investigated using TEM and SEM analysis, respectively. On Figure 3(a), the PANI-HCl TEM image shows the existence of short flattened nanofibers with diameter size around 50 nm. Their lengths are about 100–150 nm. On the other hand, on Figure 3(b), the PANI-PTSA morphology shows the existence of long nanofibers than those of PANI-HCl with lengths ranking from 150 to 200 nm. Their average sizes are observed to be less than 20 nm mainly in crystalline forms with smooth surfaces which proves that the use of organic doping agent (PTSA) confers a pseudo-metallic characteristic to the PANI,[27] in concordance with the earlier results of X-ray diffraction. These

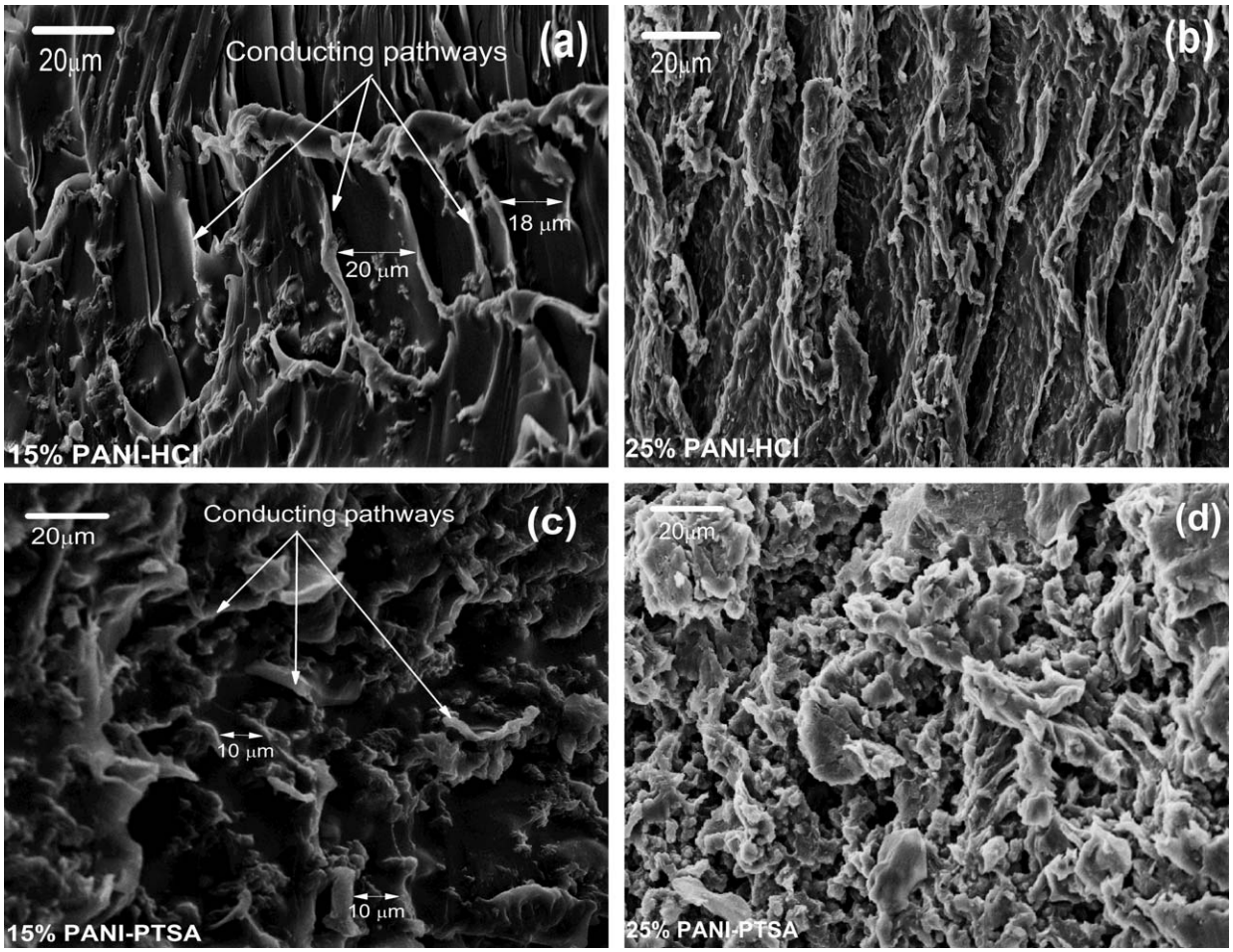

Figure 4. SEM micrographs of composite cross section for 15% and 25% PANI content, respectively: (a) and (b) PANI-HCl/PU, (c) and (d) PANI-PTSA/PU.

observations reveal the doping agent effect on the morphology of doped PANI.

The cross section micrographs of composites with 15 and 25 wt % PANI content are shown in Figures 4(a,b) and Figures 4(c,d)

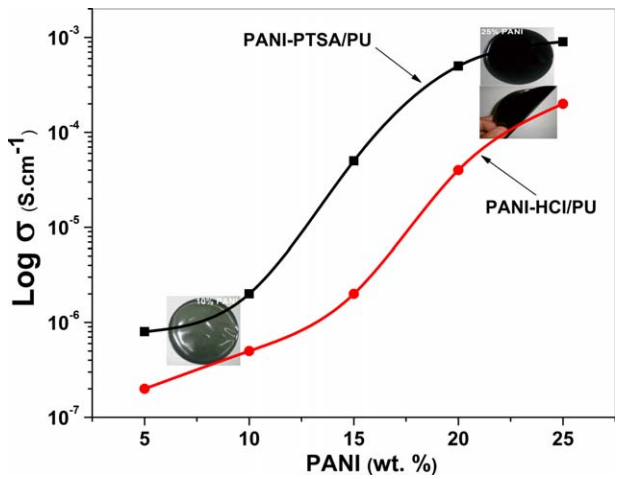

Figure 5. Evolution of conductivity with PANI content in PANI/PU flexible composite films. [Color figure can be viewed in the online issue, which is available at www.interscience.wiley.com.]

for PANI-HCl/PU and PANI-PTSA/PU composites, respectively. These images were obtained by the secondary electrons and allowed the distinction between the two phases: the PANI appears in white (conducting phase) while the aliphatic PU is in black (insulating phase).[28] For low PANI content in the composite, no pathways are observed. However, above 15 wt % PANI content, the formation of conducting pathways appear. The results are in agreement with the previous DRX observations and confirm the formation of a conductive network in the composite films with a mass fraction of doped PANI around 15% for both composites. But the distances between the conducting pathways in the cross section of composites PANI-PTSA/PU are nearest than in composites PANI-HCl/PU which will enhance the interfibers conduction hopping.[29] In terms of morphology and dispersion of doped PANI through the aliphatic PU matrix, the resulted characteristics will strongly influence the electrical and dielectric properties of composite films in the microwave band.

Electrical Measurements

The electrical conductivity of the doped PANI was measured at room temperature using a four-probe technique. The PANI-HCl and PANI-PTSA powders showed the conductivity values about 1 S cm^{-1} and 5 S cm^{-1}, respectively. These values affect the

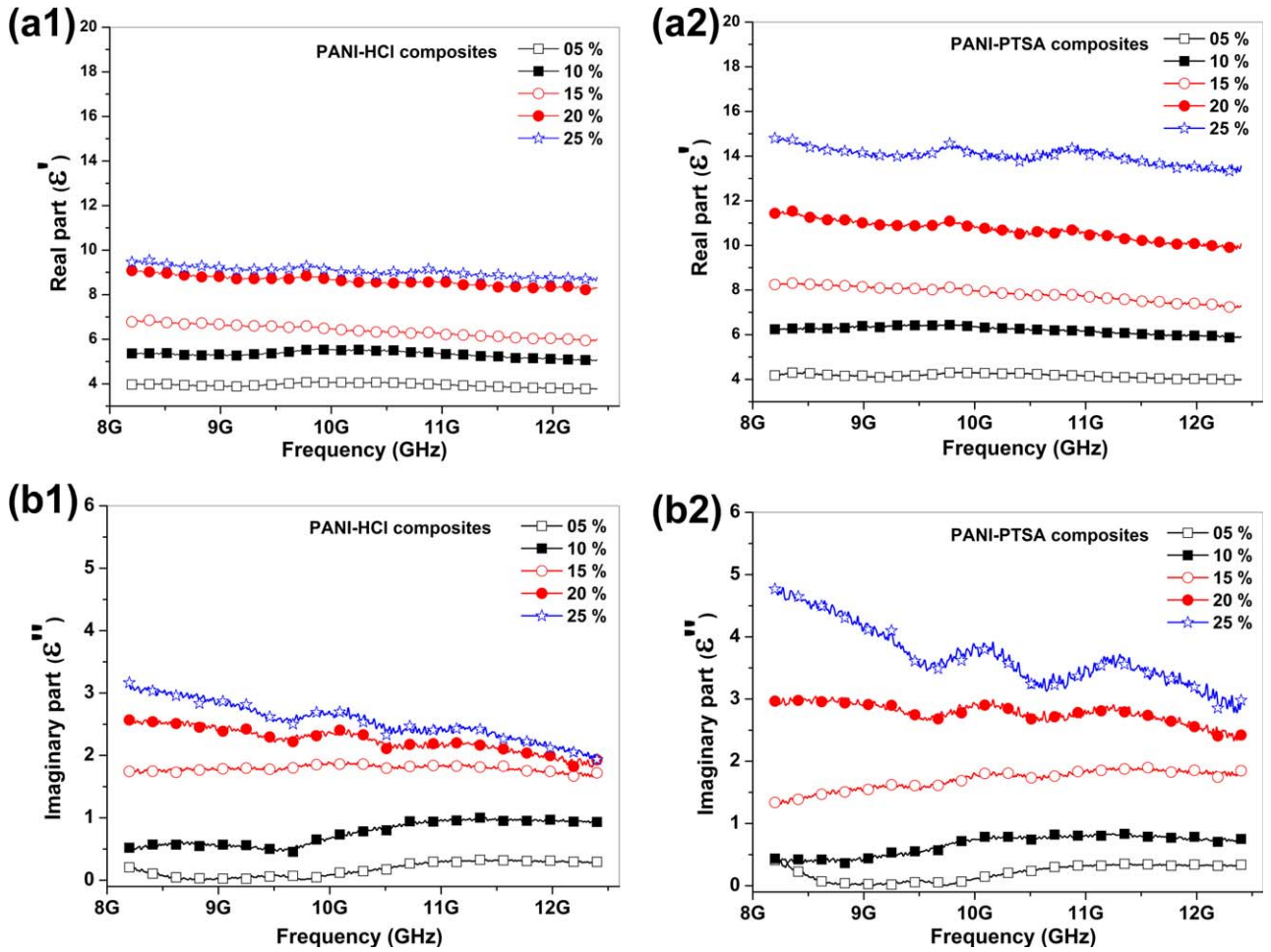

Figure 6. The composite films frequency dependence of: (a) real and (b) imaginary part of permittivity. [Color figure can be viewed in the online issue, which is available at www.interscience.wiley.com.]

electrical conductivity of the elaborate composites; thus, influence the electrical percolation thresholds as it is revealed on Figure 5.

As it can be seen, the conductivity of PANI-HCl/PU and PANI-PTSA/PU composites increases with increasing PANI loading. The plot of conductivity versus PANI content shows that the percolation thresholds of composite films are around 15 wt % of PANI-PTSA and 17 wt % of PANI-HCl. The highest values of conductivities were recorded for composite films based on PANI-PTSA. These results are in agreement with the morphologies observations and confirm that the electrical percolation threshold is dependent on dopant type and the distance between conducting pathways in composites.

Dielectric Study

The complex permittivity ($\varepsilon^* = \varepsilon' - j\varepsilon''$) can be derived from the measured reflected and transmitted scattering parameters (S_{11} and S_{21}), determined directly by the VNA and using the Nicholson-Ross and Weir method.[30] The real and imaginary parts (ε', ε'') of the complex permittivity (ε^*) characterize the storage energy ability and the dissipation of electric energy of a material from an external electric field.

From Figure 6(a,b), it is shown that, the values of dielectric constant for composites increase with increasing PANI content in both samples doped HCl and PTSA agent. However, it decreases with the frequency increasing. Comparatively to the other works,[6,31] the obtained high values of (ε') and (ε'') can be interpretated by the existence of strong polarization in polyaniline generated from the presence of polaron/bipolaron and the higher crystallinity degree of PANI-PTSA compared with PANI-HCl.[32] When the frequency increases, the dipoles present in the system cannot reorient themselves along with the applied electric field and the dielectric constant decreases. Furthermore, with increasing PANI content from 5 to 25 wt %, the composite films become more conductive and the values of (ε', ε'') are jumped from (4 and 0.2) to (9 and 2.5) for PANI-HCl/PU composites respectively. While for PANI-PTSA/PU composites, the values of (ε', ε'') are increased significantly from (4 and 0.2) to (15 and 3.5), respectively. These higher values of permittivity obtained with PANI-PTSA/PU composite films can be attributed to the smaller distance between the conducting pathways which are formed within PANI-PTSA nanofibers resulting a homogeneous and high dispersion quality compared with that of PANI-HCl in the insulating PU matrix. Moreover, the gained

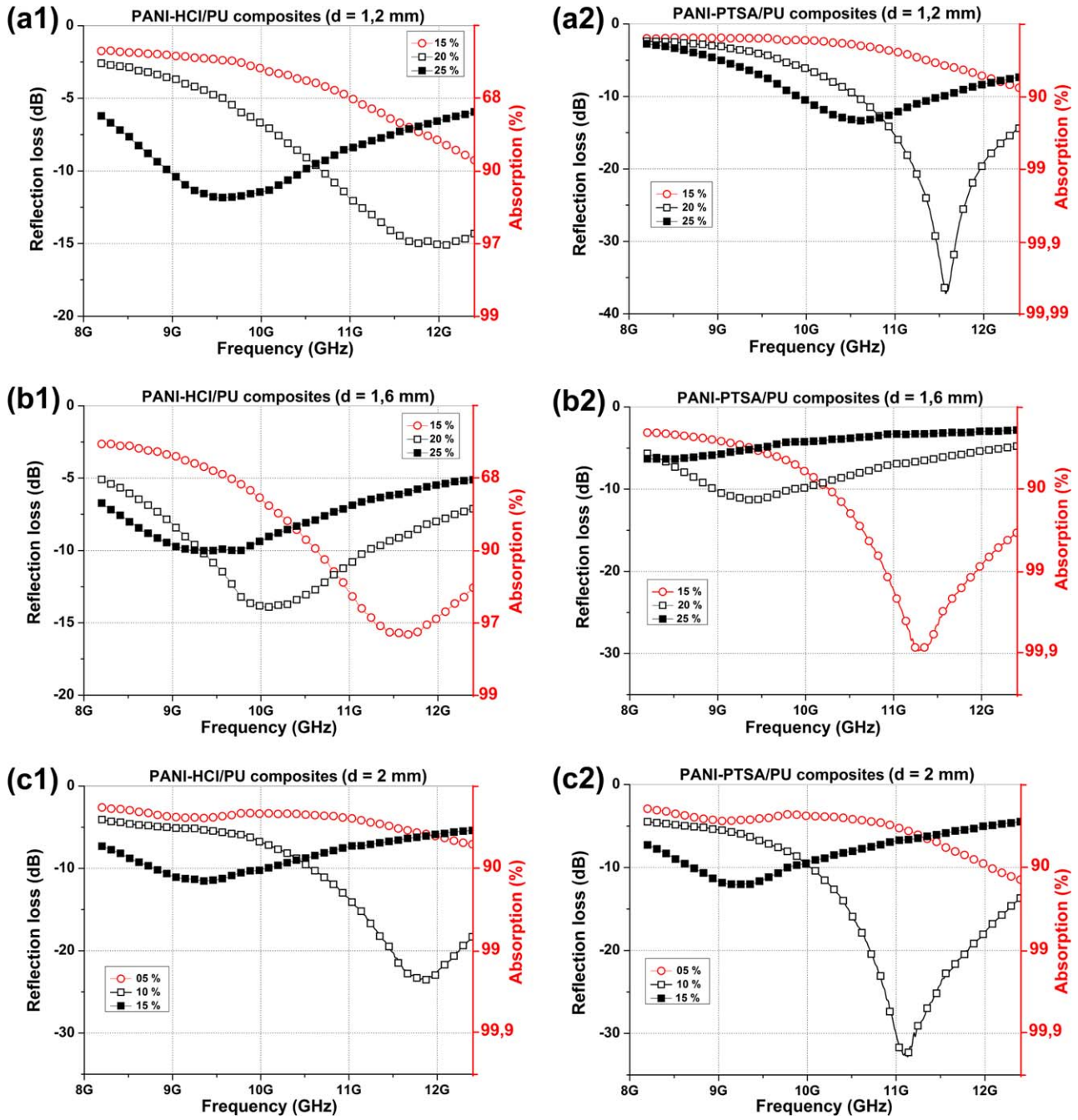

Figure 7. The composite films frequency dependence of $RL_{(dB)}$ with different type dopants, PANI contents and film thicknesses: (a) 1.2 mm, (b) 1.6 mm, and (c) 2 mm. [Color figure can be viewed in the online issue, which is available at www.interscience.wiley.com.]

dispersion of PANI in PU matrix can also lead to a large capacitance of the system mainly caused by the interfacial polarization and which will by its turn favors the ohmic loss of incident energy conducting to an improvement of waves absorption.[33] Consequently, dopant type (organic PTSA or mineral HCl), conductivity and particles size of doped PANI affect significantly the composite dielectric properties and will influence microwave absorption in X band.

Microwave Absorbing Properties

When an electromagnetic wave is transmitted through a medium, its absorption property depends on: permittivity, specific surface area, and the wave frequency.[7] The efficiency of the absorber is linked to the physical properties of filler and its degree of the dispersion in the polymer host. In case of single layer dielectric absorber, the reflection loss $RL_{(dB)}$ is calculated by the measured through the measurement of the complex permittivity based on the basis of the transmission line theory.[31,34]

$$Z_{\text{int}}/Z_0 = \sqrt{\left(\frac{1}{\varepsilon' - j\varepsilon''}\right)} \quad \tanh\left(\left(j\frac{2\pi.f.d}{c}\right)\sqrt{\varepsilon' - j\varepsilon''}\right) \qquad (1)$$

Table II. Relationship Between PANI Content, Thickness, and the Minimum Reflection Loss of Composite Films

Sample compositions	PANI rate (%)	DC conductivity (S cm^{-1})	Thickness (mm)	Minimum reflection loss
PANI-PTSA/PU	20	6.10^{-4}	1.2	−37 dB at 11.6 GHz
PANI-HCl/PU		4.10^{-5}		−15 dB at 12.0 GHz
PANI-PTSA/PU	15	6.10^{-5}	1.6	−30 dB at 11.3 GHz
PANI-HCl/PU		2.10^{-6}		−16 dB at 11.6 GHz
PANI-PTSA/PU	10	2.10^{-6}	2	−32 dB at 11.1 GHz
PANI-HCl/PU		5.10^{-7}		−23 dB at 11.8 GHz

$$RL_{(dB)} = 20\log\left|\frac{(Z_{int}/Z_0 - 1)}{(Z_{int}/Z_0 + 1)}\right| \quad (2)$$

Where $RL_{(dB)}$ is the microwave reflection loss, (ε') and (ε'') are the real and imaginary parts of the complex permittivity. Z_{int} is the normalized input impedance at air absorber interface and Z_0 is the impedance of free space. f is the frequency of incident wave, d is the absorption layer thickness and c is the light velocity.

The calculated spectra of reflection loss (S_{11}) were determined by injecting in the equations (1) and (2) the data values of the real and imaginary parts (ε', ε'') of the complex permittivity obtained earlier by Nicholson-Ross and Weir method in agreement with the work of Pitman et al.[30] While the spectra of the measured reflection loss $RL_{(dB)}$ were obtained directly by the use of short-circuit on the rear face of the samples with the network analyzer and measuring the (S_{11}) coefficient:

$$RL_{(dB)} = 20\log\ (S_{11}) \quad (3)$$

The dip in $RL_{(dB)}$ indicates the occurrences of absorption or minimal reflection of microwave power. The intensity and frequency at the minimum $RL_{(dB)}$ are linked to the thickness of samples and electromagnetic properties.[35] Figure 7 presents the composite frequency dependence of $RL_{(dB)}$ with different type dopants, PANI contents, and film thicknesses in the X band.

As it can be seen, the intensities of absorption are more important in the case of PANI-PTSA/PU films than PANI-HCl/PU for the same PANI content and thickness, which confirms the effect of dopant type, in concordance with the dielectric results and morphological properties.

Figure 7 also shows that the absorbing properties of composites depend on the PANI content. The PANI/PU composite films show an increase of the reflection loss $RL_{(dB)}$ by increasing PANI loading which results a composite conductivity proportionality. For these reasons only the composite films with PANI content above electrical percolation threshold (15, 20, and 25) with conductivity around 10^{-5} S cm^{-1} show minimal reflection of microwave at small thicknesses about 1.2 and 1.6 mm. However, it is found that the composite films with PANI content below electrical percolation threshold with lower conductivity require more thickness equal to 2 mm to absorb the electromagnetic wave in this frequency band.

Consequently, it proves that the reflection loss strongly depends on the thickness of composite films and the dip in $RL_{(dB)}$ shifts towards the low frequency by increasing film thicknesses and PANI content or conductivity. The $RL_{(dB)}$ reveals at thicknesses of 1.2, 1.6, and 2 mm, values of (−15 dB at 12 GHz), (−16 dB at 11.6 GHz) and (−23 dB at 11.8 GHz) for 20, 15, and 10 wt % PANI-HCl content respectively and (−37 dB at 11.6 GHz), (−30 dB at 11.3 GHz), and (−32 dB at 11.1 GHz) for 20, 15, and 10 wt % PANI-PTSA content, respectively. The results are summarized in the Table II.

In comparison to the references,[36,37] the explanation of these high absorption values obtained are built on three points: First, using PANI nanofibers with appropriates dopant (PTSA) has conferred a better impedance matching and has given a higher

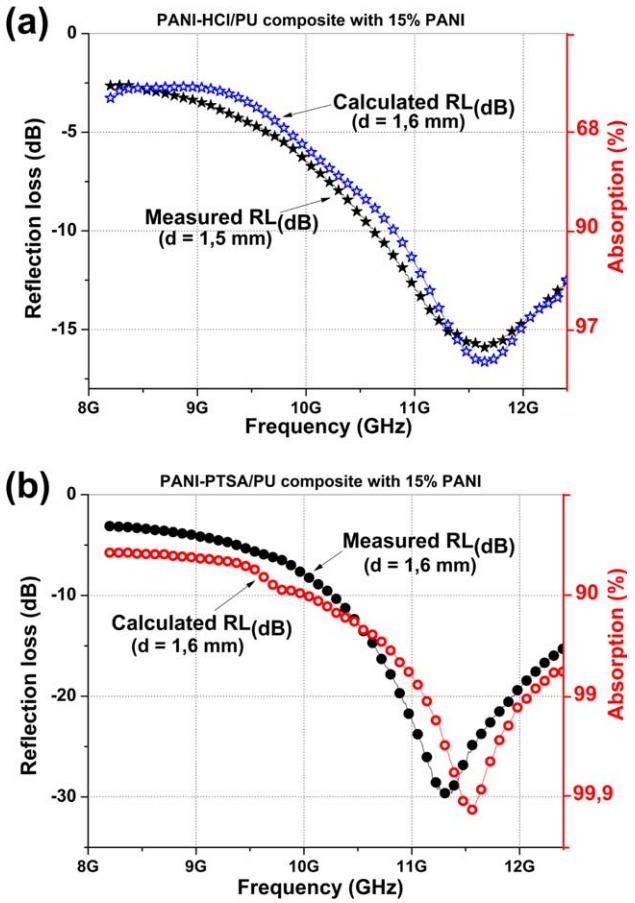

Figure 8. The comparison of measured and calculated $RL_{(dB)}$ for: (a) PANI-HCl/PU and (b) PANI-PTSA/PU composites with 15 wt % PANI content. [Color figure can be viewed in the online issue, which is available at www.interscience.wiley.com.]

dielectric constants to composite films. Second, the high level of protonation and crystallinity of PANI filler, associated to the hyperbranched aliphatic PU as polymer host has improved respectively interaction between components, conductivity and charge localization/interfacial polarization.[34] Third, the *in situ* one shot-polymerization process have contributed largely to obtain more performance of the thin films composites through preserving a flexible mechanical properties and helping to enhance microwave absorbing properties. Finally, the combination of the supra-mentioned parameters has lead to better dielectrical and microwave absorbing properties of the prepared composites without using metallic or carbon fillers.

The measured absorption spectra for both composite films PANI-HCl/PU and PANI-PTSA/PU with 15 wt % PANI content have been compared with calculated spectra in Figure 8(a,b) respectively. A good agreement between measurements and calculated curves is found. The small differences in the measured and the calculated values of reflection loss in the case of PANI-HCl/PU composites can be attributed to the surface irregularity of the absorber sample, gap between the sample and wave-guide dimensions or air gap between sample and metal short circuit.[38]

CONCLUSIONS

Organic composite microwave absorbers containing polyaniline doped with different agents were successfully prepared by in situ one-shot polymerization process in aliphatic polyurethane matrix. The PANI/PU composites characterization showed that nanostructured PANI form a continuous percolating phase dispersed in a PU matrix linked together by intra chain hydrogen bonds which affect blend morphology.

Furthermore, the nature of doping agent (organic or mineral), PANI content and thickness affect the dielectric and microwave absorbing properties of PANI/PU composite films. The results indicate that the PANI-PTSA/PU composite films exhibit higher dielectric constant in the X-band compared to PANI-HCl/PU films. For small thickness of 1.6 mm, PANI-HCl/PU composites with 15 wt % PANI content showed value of $RL_{(dB)}$ around (-16 dB at 11.6 GHz; $>97\%$ power absorption). The higher values of RL (-37 dB at 11.6 GHz and -30 dB at 11.3 GHz; $>99.9\%$ power absorption) were obtained with PANI-PTSA/PU composites for 20 and 15 wt % PANI at 1.2 and 1.6 mm respectively. The shifts of the attenuation peak in microwave absorbing properties of composites are due to the increase of the PANI content in blends and films thicknesses. The microwave absorbing properties can be modulated simply by controlling the PANI content and thickness of the composite films for the required frequency bands. This class of lightweight PANI/PU flexible composite films based on PANI nanofibers and aliphatic PU is promising microwave absorbing material for aeronautical and aerospace applications.

ACKNOWLEDGMENTS

The authors wish to express their gratitude to all researchers of EMP (Algeria) and EMD-SAGE (France) for their experimental assistance and discussions.

REFERENCES

1. Fletcher, A.; Gupta, C. M.; Dudley, L. K.; Vedeler, E. *Compos. Sci. Technol.* **2010**, *70*, 953.
2. Belaabed, B.; Wojkiewicz, J.-L.; Lamouri, S.; El Kamchi, N.; Redon, N. *Polym. Adv. Technol.* **2012**, *23*, 1194.
3. Christopher, J.; Klemperer, V.; Maharaj, D. *Compos. Struct.* **2009**, *91*, 467.
4. Oh, J.-H.; Oh, K.-S.; Kim, C.-G.; Hong, C.-S. *Composites, Part B.* **2004**, *35*, 49.
5. White, D. R. J. A Handbook on Shielding Design Methodology and Procedures; Interference Control Technologies: U.S.A, **1987**.
6. Abbas, S. M.; Chandra, M.; Verma, A.; Chatterjee, R.; Goel, T. C. *Compos. Part A.* **2006**, *37*, 2148.
7. Belaabed, B.; Wojkiewicz, J.-L.; Lamouri, S.; El Kamchi, N.; Lasri, T. *J. Alloys Compd.* **2012**, *527*, 137.
8. Fox, R. T.; Wani V.; Howard, K. E.; Bogle, A.; Kempel, L. *J. Appl. Polym. Sci.* **2008**, *107*, 2558.
9. Hoang, N. H.; Wojkiewicz, J.-L.; Miane, J. L.; Biscarro, R. S. *Polym. Adv. Technol.* **2007**, *18*, 257.
10. Satheesh Kumar, K. K.; Geetha, S.; Trivedi, D. C. *Curr. Appl. Phys.* **2005**, *5*, 603.
11. Reddy, K. R.; Lee, K. P.; Gopalan, A. I. *Colloids Surf. A.* **2008**, *320*, 49.
12. Wang, Y.; Jing, X. *Polym. Adv. Technol.* **2005**, *16*, 344.
13. Pud, A.; Ogurtsov, N.; Korzhenko, A.; Shapoval, G. *Prog. Polym. Sci.* **2003**, *28*, 1701.
14. Pinho, M. S.; Gregori, M. L.; Nunes, R. C. R.; Soares, B. G. *Eur. Polym. J.* **2002**, *38*, 2321.
15. Park, K. Y.; Lee. S. E.; Kim, C. G.; Han, J. H. *Compos. Sci. Technol.* **2006**, *66*, 576.
16. Stejskal, J.; Gilbert, R. G. *Pure Appl. Chem.* **2002**, *74*, 857.
17. Gairola, S. P.; Verma, V.; Kumar, L.; Dar, M. A.; Annapoorni, S.; Kotnala, R. K. *Synth. Met.* **2010**, *160*, 2315.
18. Khanna, P. K.; Kulkarni, M. V.; Singh, N.; Lonkar, S. P.; Subbarao, V. V. V. S.; Viswanath, A. K. *Mater. Chem. Phys.* **2006**, *95*, 24.
19. Li, J.; Tang, X.; Li, H.; Yan, Y.; Zhang, Q. *Synth. Met.* **2010**, *160*, 1153.
20. Fan, M.; He, Z.; Pang, H. *Synth. Met.* **2013**, *166*, 1.
21. Hussain, A. M. P.; Kumar, A. *Bull. Mater. Sci.* **2003**, *26*, 329.
22. Jena, K. K.; Chattopadhyay, D. K.; Raju, K. V. S. N. *Eur. Polym. J.* **2007**, *43*, 1825.
23. Umare, S. S.; Chandure, A. S. *Chem. Eng. J.* **2008**, *142*, 65.
24. Luo, J.; Wang, X.; Li, J.; Zhao, X.; Wang, F. *Polymer.* **2007**, *48*, 4368.
25. Saini, P.; Arora, M. *J. Mater. Chem. A.* **2013**, *1*, 8926.
26. Han, Y.-G.; Kusunose, T.; Sekino, T. *Synth. Met.* **2009**, *159*, 123.
27. Sinha, S.; Bhadra, S.; Khastgir, D. *J. Appl. Polym. Sci.* **2009**, *112*, 3135.
28. Roicchman, Y.; Titelman, G. I.; Silverstein, M. S.; Siegmann, A.; Narkis, M. *Synth. Met.* **1999**, *98*, 201.

29. Rubinger, C. P. L.; Costa, L. C.; Faez, R.; Martins, C. R.; Rubinger, R. M. *Synth. Met.* **2009**, *159*, 523.
30. Pitman, K. C.; Lindley, M. W.; Simkin, D.; Cooper, J. F. *IEE Proc F.* **1991**, *138*, 223.
31. Oyharçabal, M.; Olinga, T.; Foulc, M.-P., Lacomme, S.; Gontier, E.; Vigneras, V. *Compos. Sci. Technol.* **2013**, *74*, 107.
32. Yao, Y.; Jiang, H.; Wu, J.; Gu, D.; Shen, L. *Procedia Eng* **2012**, *27*, 664.
33. Singh, K.; Ohlan, A.; Bakhshi, A. K.; Dhawan, S. K. *Mater. Chem. Phys.* **2010**, *119*, 201.
34. Micheli, D.; Apollo, C.; Pastore, R.; Marchetti, M. *Compos. Sci. Technol.* **2010**, *70*, 400.
35. Phang, S. W.; Daik, R.; Abdullah, M. H. *Thin Solid Films.* **2005**, *477*, 125.
36. Ting, T. H.; Jau, Y. N.; Yu, R. P. *Appl. Surf. Sci.* **2012**, *258*, 3184.
37. Açıkalın, E.; Atıcı, O.; Sayıntı, A.; Çoban, K.; Erkalfa, H. *Prog. Org. Coat.* **2013**, *76*, 972.
38. Singh, P.; Babbar, V. K.; Razdan, A.; Srivastava, S. L.; Goel, T. C. *Mater. Sci. Eng. B.* **2000**, *78*, 70.